J. Fluid Mech. (1971), *vol.* 48, *part* 3, *pp.* 605–624
Printed in Great Britain

Centrifugal convection and its effect on the asymptotic stability of a bounded rotating fluid heated from below

By G. M. HOMSY† AND J. L. HUDSON
Department of Chemical Engineering
University of Illinois, Urbana

(Received 13 July 1970 and in revised form 1 February 1971)

Centrifugally driven circulations in a rapidly rotating cylinder of fluid heated differentially in the vertical are considered. Boundary-layer solutions obtained previously are extended to include large diameter/height aspect ratios and a centrifugal acceleration of the same magnitude as that of gravity. The ratio of convective to conductive heat transfer is small in the region of parameter space considered. The effect of the circulations on the asymptotic stability of a fluid heat from below and subjected to Coriolis force is then considered. Away from the side wall of the cylinder the basic state circulation increases the critical Rayleigh number at which gravitational instabilities occur; however, a destabilization near the side wall is possible.

1. Introduction

When a rotating fluid is heated uniformly from below, solid body rotation cannot occur regardless of how small the imposed vertical temperature difference may be; motion relative to solid body rotation is produced by the coupling of the vertical density gradient and the centrifugal acceleration. Centrifugally produced convection must occur in order to balance the body forces in the radial direction. Such flows in a right circular cylinder rotating rapidly about its vertical axis have been analyzed by Barcilon & Pedlosky (1967*b*) and by Homsy & Hudson (1969) (hereafter referred to as I). Boundary-layer solutions have been obtained for limited regions of parameter space. In this paper we extend the treatment of I. We also investigate the effect of the centrifugally produced convection on the onset of gravitational instabilities in a cylinder by performing a linear stability analysis in which the basic state is that determined in the first part of this paper.

The dimensionless temperature and velocity fields of the basic state, and therefore the Nusselt number for the heat transferred between the horizontal surfaces, depend on five parameters: $\sigma = \nu/\kappa$ (Prandtl number); $\epsilon = \nu/2\omega h^2$ (Ekman number); $\gamma = a/h$ (aspect ratio); $A = g/\omega^2 a$ (acceleration ratio, or inverse Froude number); $\beta = \alpha\Delta T/8$ (thermal Rossby number). The notation corresponds to that used in I. h and a are the cylinder half-height and radius, respectively, $\alpha\Delta T$ the product of the coefficient of thermal expansion and the

† Present address: Department of Chemical Engineering, Stanford University, Stanford, California 94305.

imposed vertical temperature difference, ω the cylinder angular velocity, and ν, κ, and g have their usual meanings.

Barcilon & Pedlosky have treated the region $\beta, \epsilon \ll 1$,

$$A \gg 1, \gamma = O(1), O(1) \leqslant \gamma A \sigma \beta / \epsilon^{\frac{1}{2}} < \infty,$$

i.e. the first-order effects of a small but non-zero ratio of centrifugal to gravitational accelerations. The most interesting features in this parameter range include vertical symmetries (which disappear if higher-order effects are considered), the disappearance of the Ekman suction effect for large $\gamma A \sigma \beta \epsilon^{-\frac{1}{2}}$, and the similarities between the boundary-layer structure and the dynamics in this inherently non-linear problem and that obtained in the unified theory of stratified rotating flows (Barcilon & Pedlosky 1967*a*). In addition, the 'similarity' solution was shown to be physically inadmissible in this region of parameter space.

In I, we have treated the region $\beta, \epsilon, A \ll 1, 1 \leqslant \gamma \leqslant O(\epsilon^{-\frac{1}{6}}), \lambda = \sigma \beta \epsilon^{-\frac{1}{2}} \leqslant O(1)$, where we were restricted to $\gamma = O(1)$ in the case of insulated side walls. The parameter λ is the ratio of thermal convection to conduction in the interior region of the cylinder. The results obtained were more extensive than those of Barcilon & Pedlosky since the interior energy equation becomes linear for $A/\gamma \ll 1$. In §2 of this paper, we present further results for region β, $\epsilon \ll 1$, $A \ll (\lambda\gamma)^{-1}$, $\gamma \gg 1$, $\lambda\gamma \leqslant O(1)$, i.e. for large aspect ratios but small λ, so that the last condition holds. The similarity solution is found to be valid over large interior regions of the fluid, but in general cannot be used alone to calculate a Nusselt number. It may be noted that the parameter region $\gamma \gg 1, A = O(1)$, is of most relevance to experimental studies; for most moderate Prandtl number fluids, $\lambda\gamma \ll 1$. Thus the analysis in §2 relaxes the previous conditions on A.

We have treated the asymptotic stability of a bounded rotating cylinder of fluid heated from below in a previous paper (Homsy & Hudson 1971, hereafter referred to as II); it was assumed that the stratification was linear, i.e. the basic state was one of solid body rotation with heat being transferred only by conduction. This assumption has been made by all previous investigators (see, for example, Chandrasekhar 1961 and Niiler & Bisshopp 1965) and is suitable if the Froude number is sufficiently small. In II, a boundary-layer formulation of the stability problem was presented. It was shown that for small Ekman numbers, cylinders of aspect ratio $\gamma > 1$ may be considered infinite in extent. The asymptotic results were extended to include higher-order terms. Furthermore, the instability was shown to be due to energy conversions in the interior regions of the fluid, with dissipation in the Ekman layers producing second-order effects. It is the assumption of a conductive basic state (solid body rotation) which we wish to relax here. We consider gravitational instabilities in a rotating fluid by linearizing the equations around the convective basic state which is obtained in the first part of this paper. Many of the features of the analysis in II carry over to the present case. In our treatment of the stability of the convective basic state, we will limit ourselves to the first-order asymptotic problem, and consider instabilities due to the buoyancy mechanism alone. In order to relate this study to previous stability analyses, we use the dimensionless parameters which were used in II. These are related to the parameters introduced above: $r_0 = a/d = \frac{1}{2}\gamma$ (aspect ratio);

$E = \nu/2\omega d^2 = \frac{1}{4}\epsilon$ (Ekman number); $R = g\alpha\Delta T d^3/\nu\kappa = 16\beta A\gamma\sigma/\epsilon^2$ (Rayleigh number); $\sigma S = \nu g\alpha\Delta T/4\kappa\omega^2 d = RE^2$ (stratification parameter).

In § 3 the stability equations are developed for the asymptotic case, $E \to 0$. The main effect of the centrifugally driven basic state on the stability problem appears as a distortion of the vertical temperature gradient. The stability of the similarity profile is determined in § 4, and the regions near the cylinder side walls are treated more approximately in § 5. The results are discussed in relation to recent experimental results in § 6.

2. The basic state for large aspect ratio

When the Ekman number is small (large Taylor number) boundary layers form on all the surfaces of the cylinder. A thermal wind arising from a balance of Coriolis and centrifugal forces occurs in the inviscid core. Horizontal Ekman layers control the inviscid axial flow for the region of parameter space considered in I.

For stable stratification the fluid flows radially inward in the upper Ekman layer, downward in the inviscid core, outward in the lower Ekman layer. It is channelled upward in the side boundary layer and there is also a closed circulation in the inner Stewartson layer. Heat is thus transferred from the warm upper surface to the cool lower surface by both convection and conduction. The ratio of convection to conduction in the inviscid core is given by the parameter $\lambda = \sigma\beta/\epsilon^{\frac{1}{2}}$.

The dimensionless temperature in I is defined using a scale $\frac{1}{2}\Delta T = \frac{1}{2}(T_a - T_b)$ where T_a and T_b are the temperatures of the top and bottom surfaces of the cylinder, respectively. The parameter β defined above is then $\alpha(T_a - T_b)/8$. We were concerned in I with stable stratification so that $\Delta T = T_a - T_b > 0$. However, the solutions in I also hold for unstable stratification with all parameters and dimensionless variables which have a factor ΔT becoming negative. For ease of presentation and in order to keep the basic state analysis on a common basis with that in I, we consider a stable stratification in § 2. For the stability study in § 3, 4 and 5, we use a scale $|\Delta T|$ and add minus signs to the basic state solution where necessary. Thus the stability analysis is on a common basis with II.

The largest component of the temperature satisfies a non-linear energy equation and this temperature must satisfy the imposed boundary conditions at the horizontal surfaces. The boundary conditions at the side wall are obtained by a detailed treatment of the side-wall boundary layers. The largest component, θ, of the interior dimensionless temperature satisfies the following boundary-value equation which was derived in I:

$$-\lambda\left(2^{\frac{1}{2}} + \frac{A}{2^{\frac{3}{2}}\gamma}\int_{-1}^{1}\left(\frac{1}{r}\frac{\partial}{\partial r} r \frac{\partial\theta}{\partial r}\right) dz\right)\frac{\partial\theta}{\partial z} = \nabla_\gamma^2\theta, \tag{2.1}$$

$$\theta = \pm 1, \quad z = \pm 1, \tag{2.2}$$

$$\theta = z, \quad r = 1 \quad \text{(conducting walls)}, \tag{2.3}$$

$$\frac{\partial\theta}{\partial r} = -\frac{\lambda\gamma}{2^{\frac{1}{2}}}\frac{\partial\theta}{\partial z}, \quad r = 1 \quad \text{(insulated walls, } A > \epsilon^{\frac{1}{8}}\text{)}, \tag{2.4a}$$

$$\frac{\partial\theta}{\partial r} = -\frac{\lambda\gamma}{2^{\frac{1}{2}}}\left[\frac{\partial\theta}{\partial z} + 2^{\frac{1}{2}}\lambda\gamma\frac{d}{dz}\left\{\frac{\partial\theta}{\partial z}\int_{\infty}^{0}\hat{\psi}^2(\rho,z)\,d\rho\right\}\right], \quad r = 1 \quad \text{(insulated walls, } A < \epsilon^{\frac{1}{6}}\text{)}. \tag{2.4b}$$

Here

$$\nabla_\gamma^2 = \frac{\partial^2}{\partial z^2} + \frac{1}{\gamma^2}\frac{1}{r}\frac{\partial}{\partial r}r\frac{\partial}{\partial r}, \tag{2.5}$$

and $\hat{\psi}$ is the lowest-order closed circultion within the Stewartson $\epsilon^{\frac{1}{3}}$ layer. v', the dimensional interior tangential velocity with respect to a rotating co-ordinate system, is given by

$$v' = \tfrac{1}{4}\alpha\Delta T\omega r'\theta, \tag{2.6}$$

where r' is the dimensional radial co-ordinate. The interior axial velocity is independent of axial position, and is smaller than v' by a factor of $O(\epsilon^{\frac{1}{2}})$. The interior radial velocity is zero to $O(\epsilon)$ since the flow is axisymmetric. The first correction to θ is $O(\epsilon^{\frac{1}{3}})$ for both insulating and conducting side walls (Homsy 1969).

For a radially unbounded system without side walls, a similarity solution can be obtained in which the temperature is independent of radial position. Heat transferred to the fluid from the hot upper surface is less than that transferred out at the cold lower surface. A net amount of heat enters the system from an infinite radial position in order to satisfy an overall energy balance. If in a radially bounded system the side walls are perfectly conducting, there is again less heat transferred in through the cylinder top than transferred out through the bottom and the overall energy balance is satisfied by the transfer of heat through the cylinder side wall. The overall Nusselt numbers governing heat transfer through the cylinder top and bottom approach those obtained from the similarity solution as the cylinder aspect ratio γ becomes large. When the side walls are insulated, the Nusselt numbers for the cylinder top and bottom cannot approach the similarity values as γ becomes large since the overall energy balance would not be satisfied. The behaviour for large γ was not determined in I since the semi-numerical solutions for an insulated side wall were restricted to $\gamma = O(1)$. It is of interest to determine if the similarity solution holds over any region of the cylinder as the aspect ratio is increased. It will be seen below that the similarity solution does hold away from the side wall (in the parameter region under consideration) for a cylinder of large aspect ratio regardless of the side-wall boundary condition.

For large γ, (2.1), (2.2) admit a similarity solution valid to within $O(\gamma^{-1})$ of the side walls. In the region $1-r = O(\gamma^{-1})$, radial diffusion must also be important in order to allow the boundary conditions at $r = 1$ to be satisfied. On this hypothesis, in these regions,

$$\gamma^{-2}\frac{1}{r}\frac{\partial}{\partial r}r\frac{\partial}{\partial r} \sim \frac{\partial^2}{\partial z^2} = O(1),$$

which suggests the stretching of the radial co-ordinate as

$$\eta = (1-r)\gamma. \tag{2.7}$$

Thus we seek the solutions of the form

$$\theta(r,z) = \theta^*(z) + \hat{\theta}(\eta,z). \tag{2.8}$$

Here $\theta^*(z)$ denotes the similarity solution, discussed shortly, and $\hat{\theta}(\eta, z)$ denotes a correction (not necessarily small) to θ^* in a layer near the sides. Thus we must have $\lim_{\eta\to\infty} \hat{\theta} = 0$. The thickness of this layer is $O(\gamma^{-1})$, and is therefore thicker than any of the viscous layers near these same walls. (In this scaling the outer Stewartson layer has a dimensionless thickness of $O(\epsilon^{\frac{1}{4}}/\gamma)$.)

Most of the analysis will be for the linear boundary conditions, (either (2.3) or (2.4*a*)); indeed there is good reason to believe that (2.4*a*) is the proper boundary condition for $A = O(1), \lambda \ll 1, \lambda\gamma \leqslant O(1)$ (see Barcilon & Pedlosky 1967*b*, p. 683). Assuming (2.4*a*) valid for $A = O(1)$, the restriction of the solutions developed below becomes $A \ll (\lambda\gamma)^{-1}$, which for most experimental situations represents a milder restriction than $A \ll 1$.

The similarity solution

With the assumed form (2.8) the problem for θ^* is quite simple, viz.

$$-2^{\frac{1}{2}}\lambda D\theta^* = D^2\theta^*, \tag{2.9a}$$

$$\theta^* = \pm 1, \quad z = \pm 1, \tag{2.9b}$$

where $D = d/dz$. We choose the similarity solution to satisfy the isothermality conditions at the top and bottom surfaces. It is, of course, incapable of satisfying either (2.3) or (2.4). Note that in posing (2.9) we have placed no restriction on A/γ. The similarity solution has the closed form representation,

$$\theta^* = \frac{\cosh(2^{\frac{1}{2}}\lambda) - \exp(-2^{\frac{1}{2}}\lambda z)}{\sinh(2^{\frac{1}{2}}\lambda)}. \tag{2.10}$$

In addition, we shall later require a representation in terms of the expansion functions $\chi_n(z)$, (see I, §6),

$$\theta^* = z + 2^{\frac{1}{2}}\lambda \sum_{n=1}^{\infty} a_n \beta_n^{-2} \chi_n(z). \tag{2.11}$$

The notation corresponds to that in I,

$$\left.\begin{aligned} \chi_n(z) &= \exp(-\lambda z/2^{\frac{1}{2}}) \sin \tfrac{1}{2}n\pi(z+1), \\ \beta_n^2 &= \tfrac{1}{2}\lambda^2 + (\tfrac{1}{2}n\pi)^2, \\ a_n &= \int_{-1}^{1} \exp(2^{\frac{1}{2}}\lambda z)\chi_n(z)\,dz. \end{aligned}\right\} \tag{2.12}$$

Lastly, we note the expansion of θ^* in terms of λ,

$$\theta^* = z + 2^{-\frac{1}{2}}\lambda(1-z^2) + \tfrac{1}{3}\lambda^2 z(z^2-1) + \ldots. \tag{2.13}$$

If there were no convection, i.e. $\lambda = 0$, the temperature profile would be linear between the top and bottom of the cylinder. It can be seen from (2.13) (stable stratification) that the effect of convection is to sweep the isotherms down toward the cooler bottom surface. From (2.10), (2.11) or (2.13) it can be shown that as λ increases the temperature gradient decreases at the upper surface and increases at the lower surface. For an unstable stratification the flow in the inviscid core would be up and the isotherms would be squeezed toward the upper surface. This

squeezing of the isotherms has an effect on the critical Rayleigh number for a layer heated from below, as will be seen later in this paper.

The Nusselt number for this profile is

$$Nu(\pm 1) = \frac{2^{\frac{1}{2}}\lambda \exp(\mp 2^{\frac{1}{2}}\lambda)}{\sinh(2^{\frac{1}{2}}\lambda)}, \tag{2.14}$$

which was found in I to correspond to the solution of the full problem for a conducting side wall as $\gamma \to \infty$.

The correction fields

The correction fields are seen to satisfy

$$\left(\frac{\partial^2}{\partial \eta^2} + \frac{\partial^2}{\partial z^2}\right)\hat{\theta} = -2^{\frac{1}{2}}\lambda \frac{\partial \hat{\theta}}{\partial z} + O\left(A\lambda\gamma \frac{\partial^2 \hat{\theta}}{\partial \eta^2}\right), \tag{2.15}$$

$$\hat{\theta} = 0, \quad z = \pm 1, \tag{2.16a}$$

$$\hat{\theta} + \theta^* = z, \quad r = 1, \quad \eta = 0 \quad \text{(conducting)}, \tag{2.16b}$$

$$\frac{\partial \hat{\theta}}{\partial \eta} = \frac{\lambda\gamma}{2^{\frac{1}{2}}}\left(\frac{d\theta^*}{dz} + \frac{\partial \hat{\theta}}{\partial z}\right), \quad r = 1, \quad \eta = 0 \quad \text{(insulated)}, \tag{2.16c}$$

$$\hat{\theta} \to 0. \quad \eta \to \infty. \tag{2.16d}$$

We neglect the last term in (2.15) and discuss below the limitation which this imposes. A solution is written in terms of the $\chi_n(z)$, viz.

$$\hat{\theta} = \sum_{n=1}^{\infty} \phi_n e^{-\beta_n \eta} \chi_n(z).$$

This representation satisfies (2.15), (2.16a, d), and the constants ϕ_n are determined by either (2.16b) or (2.16c).

For conducting walls, (2.16b) and (2.11) yield

$$\phi_n = -2^{\frac{1}{2}}\lambda a_n \beta_n^{-2}, \tag{2.17}$$

and a uniformly valid representation for θ becomes

$$\theta(r, z) = z + 2^{\frac{1}{2}}\lambda \sum_{n=1}^{\infty} a_n \beta_n^{-2}(1 - e^{(-r-1)\gamma\beta_n})\chi_n. \tag{2.18}$$

This is seen to be the asymptotic form of the exact solution for $A/\gamma \ll 1$ (Homsy 1969).

$$\theta(r, z) = z + 2^{\frac{1}{2}}\lambda \sum_{n=1}^{\infty} a_n \beta_n^{-2}\left[1 - \frac{I_0(\beta_n \gamma r)}{I_1(\beta_n \gamma)}\right]\chi_n.$$

For insulated walls, the discussion becomes more involved. In this case the ϕ_n are solutions to the infinite set of linear algebraic equations,

$$\beta_n \phi_n = \frac{-\lambda\gamma}{2^{\frac{1}{2}}}\left(a_n + \sum_{m=1}^{\infty}\left(\phi_m + \frac{2^{\frac{1}{2}}\lambda a_m}{\beta_m^2}\right) d(m, n)\right), \tag{2.19}$$

$$d(m, n) = \int_{-1}^{1} \exp(2^{\frac{1}{2}}\lambda z)\, \chi_m' \chi_n \, dz.$$

Equation (2.19) is derived from (2.16*c*), (2.11), and the orthogonal properties of the $\chi_n(z)$. The set (2.19) is seen to be the asymptotic form of the set obtained in I, equation (7.5) for large γ. Any attempt to solve this set will encounter the same numerical difficulties in evaluation of Nusselt numbers as we encountered in I. It is possible, however, to generate an analytic solution through $O(\lambda^2)$ by perturbing either the original set (2.15)–(2.16*a*, *c*) or the linear system (2.19). The attack is straightforward, and the calculation yields,

$$\hat{\theta} = \lambda\gamma\hat{\theta}_1 + (\lambda\gamma)^2\hat{\theta}_2 + \lambda^2\gamma\hat{\theta}_3 + O(\gamma^3\lambda^3), \tag{2.20}$$

where

$$\hat{\theta}_1 = -2^{\frac{1}{2}} \sum_{n=0}^{\infty} \omega_n^{-2} e^{-\omega_n\eta} \sin\omega_n(z+1), \tag{2.21}$$

$$\omega_n = \tfrac{1}{2}(2n+1)\pi,$$

$$\hat{\theta}_2 = -\frac{16}{\pi^3} \sum_{n=1}^{\infty} \sum_{m=0}^{\infty} \frac{e^{-n\pi\eta} \sin n\pi(z+1)}{(2m+1)\,((2m+1)^2-(2n)^2)}, \tag{2.22}$$

$$\hat{\theta}_3 = \sum_{n=1}^{\infty} \left[(n\pi)^{-2} + \frac{64}{\pi^4} \sum_{m=0}^{\infty} (2m+1)^{-2}[(2m+1)^2-(2n)^2]^{-1} \right] \times e^{-n\pi\eta} \sin n\pi(z+1) + \sum_{m=0}^{\infty} \omega_m^{-2} e^{-\omega_m\eta z} \sin\omega_m(z+1). \tag{2.23}$$

We note that $\hat{\theta}_1$ is an even function of z, while $\hat{\theta}_2, \hat{\theta}_3$ are odd. Furthermore, the neglect of the last term in (2.15), necessary for the validity of these solutions, is justified if $A \ll (\lambda\gamma)^{-1}$; this is often less restrictive than $A \ll 1$. Lastly, we note that $\hat{\theta}_1$ is the asymptotic form of the solution obtained in I, equation (3.11).

Nusselt number calculation

Analytical results for the Nusselt number may be found. In the present notation,

$$Nu(\pm 1) = D\theta^*(\pm 1) + 2\gamma^{-1} \int_0^{\infty} \left.\frac{\partial\hat{\theta}}{\partial z}\right|_{z=\pm 1} d\eta. \tag{2.24}$$

We note that for conducting walls, $\hat{\theta}$ is an $O(1)$ function *uniformly* in γ as $\gamma \to \infty$. Thus for this case,

$$Nu(\pm 1) = D\theta^*(\pm 1),$$

with an error of $O(\gamma^{-1})$. This is in agreement with our previous findings in I.

For insulated walls, through $O(\lambda^2)$,

$$Nu(\pm 1) = 1 \mp 2^{\frac{1}{2}}\lambda + 2\lambda \int_0^{\infty} \left.\frac{\partial\hat{\theta}_1}{\partial z}\right|_{\pm 1} d\eta + \lambda^2 \left(2\gamma \int_0^{\infty} \left.\frac{\partial\hat{\theta}_2}{\partial z}\right|_{\pm 1} d\eta + 2\int_0^{\infty} \left.\frac{\partial\hat{\theta}_3}{\partial z}\right|_{\pm 1} d\eta + \frac{2}{3} \right). \tag{2.25}$$

The $O(\lambda)$ terms vanish for reasons discussed in I (§ 3); carrying out the indicated calculations yields

$$Nu(\pm 1) = 1 + 0{\cdot}5428\lambda^2\gamma - \tfrac{2}{3}\lambda^2. \tag{2.26}$$

Writing as in I, $Nu = 1 + S(\gamma)\lambda^2$, we obtain the asymptotic form of $S(\gamma)$, viz.

$$S(\gamma) = 0{\cdot}5428\gamma - \tfrac{2}{3}. \tag{2.27}$$

Values of $S(\gamma)$ are given in table 1, where we have compared them with the numerical results obtained in I. The agreement is good even at low γ, and indicates that the aspect ratio need only be slightly greater than 3 in order for the asymptotic theory to be applicable through $O(\lambda)^2$.

A similar analysis may be carried out for the more complicated boundary condition (2.4*b*). The result of this computation may be found in Homsy (1969),

$$S(\gamma) = 0{\cdot}578\gamma - \tfrac{2}{3}.$$

The similarity between this and (2.27) substantiates the conclusion reached in I that gravity has only a slight local effect on the flow, confined to regions near the side walls. (Note that $A = 0$ for zero gravity, and small A affects only the function θ_2 through $O(\lambda^2)$.)

γ	Numerical values from I	Asymptotic results (2·27)
1·0	0·193	−0·124
2·0	0·627	0·419
3·0	1·13	0·962
5·0	2·17	2·047
10·0	4·82	4·761
15·0	7·47	7·475

TABLE 1. The function $S(\gamma)$

Thus the similarity solution is valid over most of the cylinder for either an insulated or conducting side wall when the aspect ratio is large; the similarity solution can be used to calculate the Nusselt number when the side wall is conducting, but not if it is insulated. Indeed, for insulated walls, the flux/area through the horizontal surfaces near the sides is larger by $O(\gamma^2)$ than that through the majority of the surface. The area of this side region is smaller than the total area by a factor of γ^{-1}, and thus the contribution of the region near the side wall to the Nusselt number is $O(\gamma)$ relative to the contribution of the similarity solution.

3. Linear stability equations

We treat now the stability of a rotating cylinder of fluid heated from below and subject to centrifugal effects. As in II, the treatment will be asymptotic in the sense that the Ekman number will be assumed very small. However, because centrifugal effects are included, the basic state is not conductive and stagnant. We concentrate on strong centrifugal effects; what is meant by 'strong' will be made clear below.

At this point care must be taken in stating the mechanism of instability under discussion. The centrifugally driven basic state is susceptible to many types of instability, viz. inertial, baroclinic, shear-flow and gravitational. Of these, we restrict our attention to instabilities associated with the gravitational mechanism discussed in II. (It may be argued that this is the mechanism which dominates

in the limit of vanishing Ekman number, but this argument has limited relevance to actual experimental systems with very small but non-zero Ekman numbers.) Thus we envision a situation in which the stratification is slowly increased until small disturbances can extract the gravitational potential energy of the basic convective state at a rate sufficient to overcome the dissipation so produced. This ignores the kinetic energy of the basic state, as well as any inertial effects. As we have seen in II, this mechanism is associated with energy conversions in the interior regions of the fluid, in which to the lowest order, the potential energy release is balanced by interior horizontal dissipation. Thus we replace the entire centrifugally driven basic state, i.e. the interior fields plus many boundary-layer corrections, by its interior representation *alone*.

The solutions for the basic state which were obtained in § 2 are also valid for a fluid heated from below. However, they are not in the most convenient form since ΔT is negative; all parameters and dimensionless variables which depend on ΔT are also negative. Therefore, we redefine

$$\theta' = |\Delta T|\theta, \quad \mathbf{Q}' = \mathbf{Q}\tfrac{1}{4}\alpha|\Delta T|\omega a, \tag{3.1}$$

where θ' and $\mathbf{Q}'$ are the dimensional basic state temperature and velocity respectively. (Note that the scaling differs from § 2 by a factor of 2.) We also redefine the parameters in terms of $|\Delta T|$, or

$$\beta = \tfrac{1}{8}\alpha|\Delta T| \quad \text{and} \quad \lambda = \sigma\beta/\epsilon^{\frac{1}{2}}.$$

Thus we modify the solutions in § 2 for use in the stability calculation by applying the transformations

$$\theta \to -2\theta, \quad \lambda \to -\lambda. \tag{3.2}$$

If we then write the temperature and velocity as the sum of this basic state and small disturbances $(\mathbf{q}', T')$ and linearize in the usual manner, the linear stability equations governing the disturbances at stationary onset (see II, § 1) become,

$$\nabla . \mathbf{q}' = 0, \tag{3.3}$$

$$\mathbf{Q}' . \nabla \mathbf{q}' + \mathbf{q}' . \nabla \mathbf{Q}' + 2\omega(\mathbf{k} \times \mathbf{q}') + r'\omega^2\alpha T'\mathbf{i} - g\alpha T'\mathbf{k} = -\rho^{-1}\nabla p' + \nu\nabla^2\mathbf{q}', \tag{3.4}$$

$$\mathbf{Q}' . \nabla T' + \mathbf{q}' . \nabla \theta' = \kappa\nabla^2 T'. \tag{3.5}$$

The Boussinesq approximation extended to rapidly rotating fluids has been invoked (see I, § 2).

For the basic state, we use the scaling (3.1) while for disturbances we employ the scaling found in II to be relevant to the asymptotic problem, viz.

$$\left.\begin{aligned} \mathbf{q}' &= \mathbf{q}g\alpha|\Delta T|/2\omega, \\ p' &= p\rho_0 g\alpha|\Delta T|d, \\ T' &= T|\Delta T|, \\ z &= z'/d, r = r'/d. \end{aligned}\right\} \tag{3.6}$$

Note that the independent variables do not correspond to those used in § 2; some care is required in writing the functionality of θ and $\mathbf{Q}$. The dimensionless formulation becomes

$$\nabla . \mathbf{q} = 0, \tag{3.7}$$

$$\beta r_0[\mathbf{Q} . \nabla \mathbf{q} + \mathbf{q} . \nabla \mathbf{Q}] + \mathbf{k} \times \mathbf{q} + (A r_0)^{-1} r T \mathbf{i} - T \mathbf{k} = -\nabla p + E \nabla^2 \mathbf{q}, \tag{3.8}$$

$$\sigma \beta r_0 (\mathbf{Q} . \nabla T) + \sigma S (\mathbf{q} . \nabla \theta) = E \nabla^2 T, \tag{3.9}$$

where $\sigma = \nu/\kappa$, $\beta = \alpha |\Delta T|/8$, $A = g/\omega^2 a$, and as in II,

$$r_0 = a/d = \tfrac{1}{2}\gamma, \quad E = \nu/2\omega d^2, \quad \sigma S = \nu g \alpha |\Delta T|/4\kappa\omega^2 d = R E^2,$$

$$R = g\alpha |\Delta T| d^3/\nu\kappa.$$

In simplifying these equations, we rely heavily upon the attack taken in II, which we assume will again be adequate to describe the gravitational instabilities of the present basic state. We first show that the inertial terms are negligible, thus eliminating the possibility (for the range of β considered here) of any inertial instabilities associated with the interior basic flow. The form of $\mathbf{Q}$ is (see § 2)

$$\mathbf{Q} = (U, V, W) = (0, 2r\theta/r_0, O(E^{\frac{1}{2}})). \tag{3.10}$$

Since the radial component of $\mathbf{Q}$ is zero, the bracketed inertial terms in (3.8) contain no derivatives of $\mathbf{q}$ with respect to r. This is important since we anticipate that the interior horizontal length scale of $\mathbf{q}$ will be $O(E^{\frac{1}{3}})$, as in II. Furthermore, the largest of these bracketed terms are those involving V, and (from (3.10)) are at most $O(r_0^{-1})$, so that the inertial terms are at most $O(\beta)$. We anticipate that the first non-geostrophic component of the remainder of (3.8) will again be $O(E^{\frac{1}{3}})$ from the horizontal part of $E\nabla^2\mathbf{q}$. This non-geostrophic part is necessary to generate a continuity equation to the lowest order. Thus in order to neglect inertia to the lowest order, we must have $\beta \ll E^{\frac{1}{3}}$, which is a restriction on the validity of the basic flow itself, and poses no serious restriction under normal conditions, owing to the smallness of α.

We now show that the term $\sigma\beta r_0(\mathbf{Q} . \nabla T)$ is negligible compared to the other terms in (3.9). Because $U = 0$, the largest term in $\mathbf{Q} . \nabla T$ is $V/r(\partial T/\partial\phi) = O(T/r_0)$. From II, we had the asymptotic relation $R \to P E^{-\frac{4}{3}}$, where P is a constant; this implies that $T = O(E^{\frac{1}{3}})$ relative to the largest component of the perturbation velocity $\mathbf{q}$. This again will be the case if the first term in (3.9) may be neglected, i.e. $\sigma\beta E^{\frac{1}{3}} \ll E^{\frac{2}{3}}$, or $\sigma\beta \ll E^{\frac{1}{3}}$. This condition is met for the basic state under consideration, since the analysis in § 2 was for $\lambda \leqslant O(1)$, i.e. $\sigma\beta \leqslant O(E^{\frac{1}{2}}) < O(E^{\frac{1}{3}})$.

We will demonstrate below that the centrifugal term in (3.8) may be neglected under certain conditions. Including the centrifugal term, the simplified stability equations are

$$\nabla . \mathbf{q} = 0 \tag{3.11a}$$

$$\mathbf{k} \times \mathbf{q} + (A r_0)^{-1} r T \mathbf{i} = -\nabla \rho + E \nabla^2 \mathbf{q} + \mathbf{k} T, \tag{3.11b}$$

$$\sigma S (\mathbf{q} . \nabla \theta) = E \nabla^2 T. \tag{3.11c}$$

The boundary conditions for the disturbance quantities are

$$u = v = w = 0 \quad \text{(solid boundaries)},$$

$$T = 0, \quad z = 0, 1,$$

$$T = 0, \quad r = r_0 \quad \text{(conducting)},$$

$$\partial T/\partial r = 0, \quad r = r_0 \quad \text{(insulated)}.$$

The attack is identical to that employed in II, and will not be reproduced here. A new radial co-ordinate $x = r/E^{\frac{1}{3}}$ is introduced and the disturbances $\mathbf{q}, T, p$ are written as interior fields plus Ekman correction fields. An expansion in $E^{\frac{1}{3}}$ through $O(E^{\frac{1}{3}})$ is necessary to generate a continuity equation to the lowest order. and the resulting first-order interior problem becomes,

$$\frac{\partial w}{\partial z} = -\nabla_1^4 p - (Ar_0)^{-1} \frac{r}{x} \frac{\partial T}{\partial \phi}, \tag{3.12a}$$

$$v = \partial p/\partial x, \quad u = -x^{-1} \partial p/\partial \phi, \tag{3.12b, c}$$

$$\partial p/\partial z = \nabla_1^2 w + T, \tag{3.12d}$$

$$P\left(u \frac{\partial \theta}{\partial r} + w \frac{\partial \theta}{\partial z}\right) = \nabla_1^2 T, \tag{3.12e}$$

$$w = 0, \quad z = 0, 1. \tag{3.12f}$$

Here u, v, w, p, T are now the lowest-order interior fields, ϕ the azimuthal co-ordinate,

$$\nabla_1^2 = x^{-2} \frac{\partial^2}{\partial \phi^2} + x^{-1} \frac{\partial}{\partial x} x \frac{\partial}{\partial x},$$

and the eigenvalue $P = RE^{\frac{1}{3}}$ is to be determined.

The centrifugal term now appears in the continuity equation (3.12a) and is small if

$$A \gg mE^{\frac{1}{3}}/r_0, \tag{3.13}$$

where m is the azimuthal wave-number characterizing the disturbance periodicity in the tangential direction. The centrifugal term is zero to the lowest order if disturbances are assumed to be axisymmetric. However, since the disturbance interior radial velocity, u, also drops in magnitude by a factor of $O(E^{\frac{1}{3}})$, it is necessary to consider higher-order terms to generate the equivalent axisymmetric form of (3.12a). In this case it is more convenient to introduce a Stokes stream function for u and w. The resulting condition for neglect of the centrifugal term in (3.11b) is

$$A \gg E^{\frac{1}{3}}. \tag{3.14}$$

For axisymmetric disturbances, the inequality (3.14) is not unduly restrictive. However, (3.13) for asymmetric disturbances may not be easily met. We showed in II that small azimuthal wave-numbers may be used to predict critical Rayleigh numbers when centrifugal effects are neglected; however, the possibility of growth of a disturbance characterized by large m could not be completely ruled out. In this work we assume that the azimuthal wave-number is zero or at most of order unity.

Combining the conditions (3.13) and (3.14) on A with those required for the validity of the basic state yields

$$(\lambda\gamma)^{-1} \gg A \gg \begin{Bmatrix} E^{\frac{1}{3}}, \text{ axisymmetric,} \\ mE^{\frac{1}{3}}/r_0, \text{ asymmetric.} \end{Bmatrix} \tag{3.15}$$

These are the most restrictive conditions on A we have encountered, but are met in cases of sufficiently low Ekman number for moderate Prandtl number fluids.

We assume in this treatment that (3.15) holds, and will therefore neglect the last term of (3.12a). Thus in this approximation, centrifugal effects are of paramount importance in producing the convective basic state, but are relegated to secondary importance in determining the asymptotic stability of the fluid to gravitational instabilities. We see moreover, that the major effect of the centrifugal circulations on this mechanism of instability is a distortion of the basic state temperature gradient, cf. (3.12e). We now discuss solutions to the set (3.12) for various profiles.

4. Stability of the similarity profile

We first determine the asymptotic stability of the main interior region of the fluid, for which the basic state temperature is independent of radius and is given by the similarity profile (2.10) suitably modified for unstable stratification. For this profile, (3.12) can be combined to give a single equation for w, viz.

$$\frac{\partial^2 w}{\partial z^2} + P\frac{d\theta^*}{dz}\nabla_1^2 w + \nabla_1^6 w = 0. \tag{4.1}$$

We drop the conditions at the side walls and introduce as in II,

$$w = W(z)e^{im\phi}J_m(\alpha x). \tag{4.2}$$

The system for $W(z)$ then becomes

$$D^2W - P\alpha^2 D\theta^*(z;\lambda)W - \alpha^6 W = 0, \tag{4.3a}$$

$$D = d/dz,$$

$$W = 0, \quad z = 0, 1. \tag{4.3b}$$

which is the equivalent normal modes formulation. P is the eigenvalue which is to be determined as a function of the 'stretched' wave-number α, and λ; the latter appears parametrically in the basic state gradient. With due regard for the extra factor of 2 in the scaling of θ^*, and the change of axial co-ordinates, we apply (3.1) for heating from below to determine $D\theta^*$ as

$$D\theta^*(z;\lambda) = \frac{-2^{\frac{1}{2}}\lambda \exp\left(2^{\frac{1}{2}}\lambda(2z-1)\right)}{\sinh\left(2^{\frac{1}{2}}\lambda\right)}. \tag{4.4}$$

The eigenvalue problem (4.3), (4.4) has no general solution, but it is possible to generate approximate eigensolutions for small λ by applying the standard perturbation theory for the eigenvalues of self-adjoint systems (Courant & Hilbert 1953, p. 344). The details are given in Homsy (1969). If the lowest eigenvalue is expanded $P = P_0 + 2^{\frac{1}{2}}\lambda P_1 + 2\lambda^2 P_2 + \ldots,$

together with $D\theta^*$,

$$D\theta^* = -1 - 2^{\frac{1}{2}}\lambda(2z-1) - 2\lambda^2[\tfrac{1}{2}(2z-1)^2 - \tfrac{1}{6}] + \ldots,$$

the results of the calculation are

$$P_0 = (\pi^2 + \alpha^6)/\alpha^2, \tag{4.5a}$$

$$P_1 = 0, \tag{4.5b}$$

$$P_2 = P_0\left[\pi^{-2} + \frac{(\pi^2+\alpha^6)(16)^2}{\pi^6}\sum_{j=1}^{\infty}\frac{j^2}{(1-(2j)^2)^5}\right]. \tag{4.5c}$$

Requiring P to be minimized as a function of α yields the results, through $O(\lambda^2)$,

$$\left.\begin{aligned}\alpha &= 1{\cdot}3048(1+0{\cdot}09746\lambda^2),\\ P &= 8{\cdot}6965(1+0{\cdot}12954\lambda^2).\end{aligned}\right\} \tag{4.6}$$

These results predict an increase in P with increasing λ, i.e. the fluid in the interior region of the cylinder becomes more stable due to centrifugal effects. Reasons for this stabilization are discussed below.

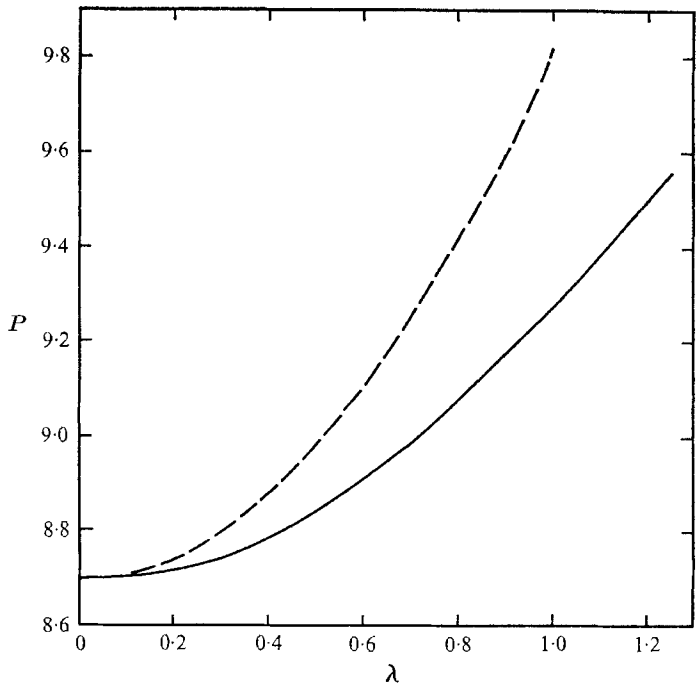

FIGURE 1. P *vs.* λ for the similarity profile. —, numerical results; - - - - -, perturbation theory, equation (4.6).

The eigenvalue problem (4.3), (4.4) was also solved numerically using a standard initial-value approach for linear eigenvalue problem (Fox 1962, p. 82). Eigenvalues were determined numerically for various values of α using a fourth-order Runge–Kutta integration scheme, and the minimum then determined. The $P(\alpha)$ curve at fixed λ is quite flat near the minimum, resulting in satisfactory values of P, but less accurate values of α at which the minimum occurs. In figure 1 we show the results of these calculations, together with the perturbation result, (4.6). It is seen that the perturbation analysis is reasonably accurate even for $\lambda = 1$, the error there being less than 6 %.

The reason for the stabilization is as follows. The profile θ^* reflects the effect of a uniform convective velocity which is upwards in the case of heating from below. The parameter λ measures the strength of this convective effect relative to conduction. As λ increases, the lower portions of the fluid tend to become homogeneous, so that the temperature contrast is felt over an effectively shallower layer

of fluid whose bottom surface is free. The asymptotic relation $R = PE^{-\frac{4}{3}}$ implies that the critical temperature difference $\Delta T_c \sim d^{-\frac{1}{3}}$, other quantities being held constant. As λ increases, the effective depth of stratified fluid decreases, thus increasing the critical Rayleigh number. This trend is slightly offset by the curvature of the gradient, which is usually a destabilizing effect, (see, for example, Watson 1968). This curvature is the origin of the second (negative) term in (4.5c), which is not of sufficient magnitude to render P_2 negative. Thus we see that the interior of the fluid is stabilized due to the unidirectional convective flow there.

5. Stability near the wall

The determination of the stability near the side wall is a more difficult task, and in this initial treatment we will consider the problem only approximately. Within $O(\gamma^{-1})$ of the wall (but still outside the viscous layers) the basic state temperature is a function of both axial distance and the stretched radial coordinate η (see §2). Stability analyses of profiles of this nature are non-existent because a radial variation of temperature implies that the fluid is not initially in mechanical equilibrium. We develop below an approximate approach which is thought to adequately represent the main effects of a more rigorous treatment. We will limit ourselves to axisymmetric disturbances, although asymmetric disturbances may be handled in a similar manner.

For axisymmetric disturbances, the energy equation (3.12e) becomes

$$Pw\left(\frac{d\theta^*}{dz}+\frac{\partial\hat{\theta}}{\partial z}\right) = \nabla_1^2 T. \tag{5.1}$$

From the results in II, the width of the convective cell is dimensionally $O(dE^{\frac{1}{4}})$, while the width of fluid over which θ has radial variation is $O(d)$. Thus the radial variation over such a convective cell is small compared to the cell width, the ratio being $O(E^{\frac{1}{4}})$. For such a slow variation, we can then assume that the fluid is locally uniform in the radial direction. We define the 'local' critical Rayleigh number as being the Rayleigh number at a given radial position calculated from the axial temperature gradient at that position. We assume that the local Rayleigh number may be calculated as for an infinite medium, although it is recognized that the solid walls will exert some constraint. This concept is on a firmer mathematical basis than might first be apparent, for if we eliminate p and T between (3.12a, d) and (5.1) we obtain

$$\frac{\partial^2 w}{\partial z^2}+P\left(\frac{d\theta^*}{dz}+\frac{\partial\hat{\theta}}{\partial z}\right)\nabla_1^2 w+\nabla_1^6 w+O(E^{\frac{3}{4}}), \tag{5.2}$$

where the $O(E^{\frac{3}{4}})$ terms are due to the radial variation of $\hat{\theta}$. Separable solutions to (5.2) of the form (4.2) exist over regions large enough to include many cells and thus allow us to drop conditions at the lateral wall, but still small enough to neglect radial variations in $\hat{\theta}$. Thus separating variables as in §4, we have

$$D^2W - P\alpha^2(D\theta^* + \partial\hat{\theta}/\partial z)W - \alpha^6 W = 0, \tag{5.3a}$$

$$W = 0, \quad z = 0, 1. \tag{5.3b}$$

For conducting walls we have

$$\frac{d\theta^*}{dz}+\frac{\partial\hat{\theta}}{\partial z}=-1, \quad \eta=0, \tag{5.4}$$

and thus the fluid immediately adjacent to the wall experiences a conductive gradient with the result that the local Rayleigh number takes its conductive value. We have not carried out any calculations for conducting walls.

We now turn to a discussion of insulated side walls, which is of more interest in a possible comparison to experiments. In this case, analytical expressions for $\hat{\theta}$ are available only through $O(\lambda^2)$; since λ is small for most cases of interest, see §6, we limit ourselves here to a perturbation analysis. We expand the local gradient, as before,

$$\frac{\partial\theta}{\partial z}=\frac{d\theta^*}{dz}+\frac{\partial\hat{\theta}}{\partial z}=-1-2^{\frac{1}{2}}\lambda(2z-1)-2\lambda^2(\tfrac{1}{2}(2z-1)^2-\tfrac{1}{6}) + (\lambda\gamma)\frac{\partial\hat{\theta}_1}{\partial z}+(\lambda\gamma)^2\frac{\partial\hat{\theta}_2}{\partial z}+\lambda^2\gamma\frac{\partial\hat{\theta}_3}{\partial z}+O(\gamma^3\lambda^3). \tag{5.5}$$

Here $\partial\hat{\theta}/\partial z$ is the gradient of the correction fields of §2, suitably modified for *unstable* stratification. It then follows that P has the expansion

$$P(\eta)=P_0+2^{\frac{1}{2}}\lambda P_1+2\lambda^2P_2+(\lambda\gamma)P_3(\eta)+(\lambda\gamma)^2P_4(\eta)+\lambda^2\gamma P_5(\eta)+O(\gamma^3\lambda^3). \tag{5.6}$$

Note the local nature of P in this case. The analysis is straightforward but lengthy. The results are as follows; P_0, P_1, P_2 are given by (4.5a, b, c) respectively. For the local contributions,

$$P_3=0, \tag{5.7}$$

$$P_4/P_0\equiv a(\eta)=\pi^{-2}\left[2e^{-\pi\eta}+3\sum_{k=1}^{\infty}\sigma_k\right], \tag{5.8a}$$

$$\sigma_k=-\frac{[(2k-1)e^{-\omega_k\eta}-(2k+1)e^{-\omega_{k-1}\eta}]^2}{((2k)^2-1)^3}, \tag{5.8b}$$

$$P_5/P_0\equiv b(\eta)=-\left[\frac{e^{-\pi\eta}}{2\pi}+\frac{2}{\pi^3}\sum_{k=0}^{\infty}(\alpha_k+\beta_k+\gamma_k)e^{-\omega_k\eta}\right], \tag{5.9a}$$

$$\alpha_k=\frac{(2k+3)^2+(2k-1)^2}{(2k+1)(2k+3)^2(2k-1)^2}, \tag{5.9b}$$

$$\beta_k=\frac{2}{(2k+1)^3}, \tag{5.9c}$$

$$\gamma_k=\frac{-4}{(2k+1)(2k+3)(2k-1)}, \tag{5.9d}$$

Thus we may write

$$P/P_0=1+\lambda^2(a(\eta)\gamma^2+b(\eta)\gamma+0{\cdot}12954). \tag{5.10}$$

The functions $a(\eta), b(\eta)$ are shown in figure 2. Note that $b(\eta)<0$, $|b(\eta)|>a(\eta)$. Therefore instabilities in regions near the wall will occur at Rayleigh numbers below those which are obtained using a conductive profile. We refer to such instabilities as 'subconductive'.

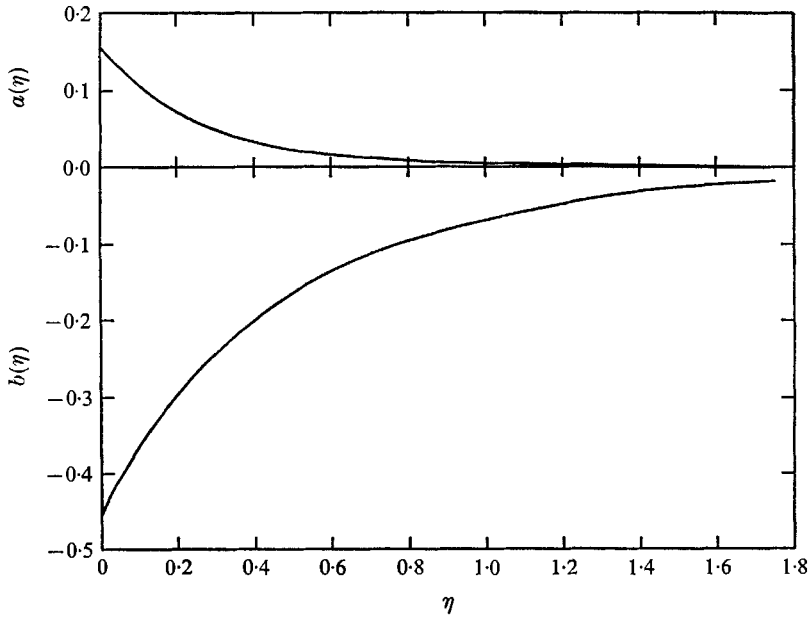

FIGURE 2. The functions $a(\eta)$, $b(\eta)$.

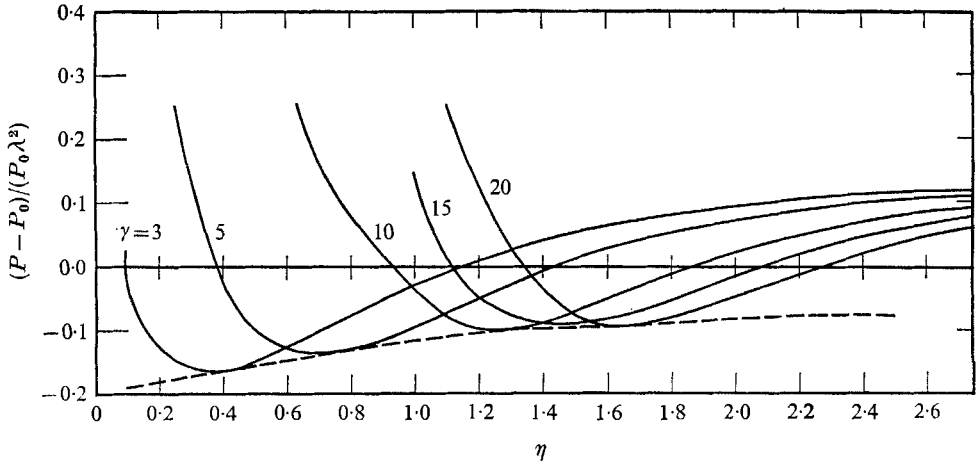

FIGURE 3. The local $O(\lambda)^2$ contribution to P.

In figure 3, values of the local $O(\lambda^2)$ contribution to P are shown as a function of radial distance for various aspect ratios. The envelope of these curves was also computed and is designated by the dotted curve. The results show two important trends. First, we note that for any aspect ratio, local subconductive instabilities are possible within the side layer near the wall. This behaviour can be explained from a consideration of the isotherms of the basic state. (The basic state for stable stratification is shown in figure 3 of I.) In the case of insulated walls, convection of heat in the side viscous layers is strongly felt as we have shown in I, with the result that the isotherms are swept downwards near the sides. This reflects the

strong effect of the rechannelling of fluid along these walls to and from Ekman layers. The net effect is again to lessen the effective depth of stratified fluid, thus stabilizing the fluid adjacent to the wall. Since the isotherms are similarily swept upwards in the interior, there must be a region removed from the wall where the isotherms are approximately conductive. It is here that the curvature of the vertical temperature gradient leads to subconductive instabilities. Obviously this effect must occur for any aspect ratio, since the basic upsweep/downsweep of isotherms occurs for any cylinder if the sides are insulated.

It is also seen from figure 3 that increasing the aspect ratio slightly decreases the magnitude of the negative correction to the Rayleigh number. This implies a less pronounced subconductive behaviour as γ increases. The approximate nature of these results is to be emphasized.

The theory is an asymptotic one, the first correction to these results being $O(E^{\frac{1}{3}})$. Including the terms of $O(E^{\frac{1}{3}})$ would entail the consideration of two effects. The first is dissipation in the Ekman layers, as discussed in II. The second is the $O(E^{\frac{1}{3}})$ correction to the basic state, which is itself an asymptotic representation.

The second major approximation was to exclude the centrifugal effects in the linear stability equations. For the axisymmetric disturbance treated here, we must have

$$E^{\frac{1}{3}} \ll A \ll (\lambda\gamma)^{-1},$$

which is satisfied if the Ekman number is sufficiently small and $\sigma = O(1)$. However, treating non-axisymmetric disturbances including centrifugal effects is clearly the next step to be taken in obtaining qualitatively useful results.

6. Discussion

Our analysis is valid for a limited range of parameter space and is not directly comparable to any published experimental results. There are, however, two studies which should be discussed. Since the theory is an asymptotic one, comparisons with experiments are qualitative.

In a study by Koschmieder (1967), a cylinder uniformly heated from below was rotated at Taylor numbers ($\tau = E^{-2}$) between zero and 10^3. Excellent photographs serve to show conclusively that axisymmetric cellular motion begins near the outer rim of the cylinder, and that adjacent cells have circulations in the same sense, with 'shear layers' between. These cell patterns are remarkably similar to those occurring in a non-rotating fluid layer with a weak radial temperature gradient, Koschmieder (1966), Müller (1966). A similar radial gradient, driven by centrifugal effects, is present near the side walls for the cases treated in §5. It is remarkable that even at very low rotational frequencies, centrifugal effects determine the sense of the circulation in the first rim roll.

The second recent study (Rossby 1969) covered a wider range of Taylor numbers, $\tau \leqslant 10^8$. Extensive measurements were made for both critical and supercritical conditions for water and mercury, and some visual observations were made with a silicone oil. Only the results for water are relevant to our analysis. Subconductive instabilities were found for all Taylor numbers greater than 5×10^4, i.e. the Rayleigh number at which measurable convection occurred

was less than that predicted by the classical linear analysis for a conductive basic state (solid body rotation). For large τ the difference between the critical Rayleigh number and that predicted by Chandrasekhar's linear theory is as much as 30 %. Also, the dependence of the Nusselt number on the Rayleigh number under supercritical conditions is different depending on whether subconductive instabilities do or do not occur. At a given Taylor number $\tau < 5 \times 10^4$ (no subconductive instabilities) the Nusselt number increases smoothly with increasing supercritical Rayleigh number. The behaviour for subconductive onset is shown in figure 4 where we have sketched Nusselt number versus Rayleigh number curves for both types of onset; this is taken from Rossby (1969, figure 12). As the Rayleigh number is raised above the critical, there is a small increase in Nusselt

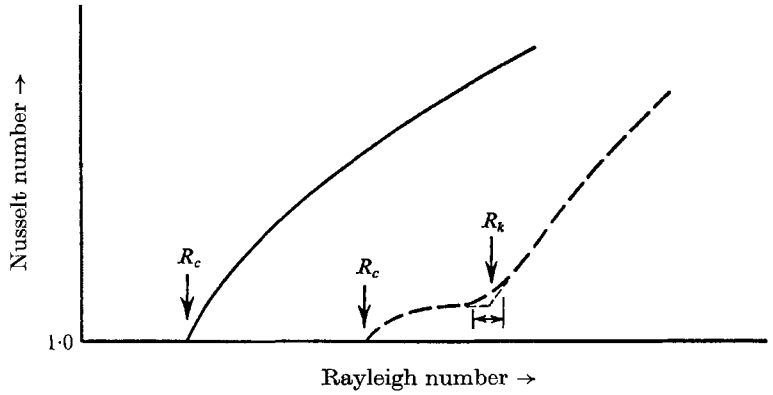

FIGURE 4. Qualitative experimental behaviour, from Rossby; —, Taylor numbers for which onset is given by conductive theory; – – –, Taylor numbers for which subconductive onset occurs.

number followed by a second break and a steeper increase thereafter. We have replotted Rossby's original data in figure 5. R_c and R_k are shown as functions of the Taylor number where R_c and R_k are respectively the critical Rayleigh number and the Rayleigh number at which the second break occurs. The R_c, of course, reproduce Rossby's marginal stability curve (Rossby 1969, figure 11) and the R_k fall approximately on the linear stability curve of Chandrasekhar.

There are several possible explanations for this type of dependence of the Nusselt number on the Rayleigh number. This behaviour is characteristic of systems which first become unstable to oscillatory modes (Chandrasekhar 1961, p. 142), although this is an unlikely explanation in this case since all available theoretical evidence indicates that for sufficiently high Prandtl number fluids onset is stationary and given by linear theory (cf. Chandrasekhar 1961, Veronis 1968, Küppers & Lortz 1969). It is also possible that the behaviour is caused by a finite-amplitude disturbance as pointed out by Rossby. Another explanation of the data is that the initial increase in the Nusselt number was caused by centrifugal circulations alone, a possibility which was suggested by Koschmieder (1967, p. 224). Finally, the subconductive behaviour found by Rossby may have been caused by the lowering of the critical Rayleigh number by centrifugal circulations as discussed in the present paper. We show below that the behaviour

indicated in figures 4 and 5 is generally in qualitative agreement with the predictions of this paper. Limitations on the region of parameter space over which our analysis is valid preclude a quantitative comparison with Rossby's data. We have tabulated experimental Taylor numbers, critical Rayleigh numbers, and the dimensionless parameters A, λ, γ in table 2; these were calculated from Rossby's raw numerical data. The parameter λ, which is the ratio of convective to conductive heat transfer in the inviscid core of the basic state, is reasonably constant and extremely small, viz. $O(10^{-3})$ for most cases. According to our analysis, at any

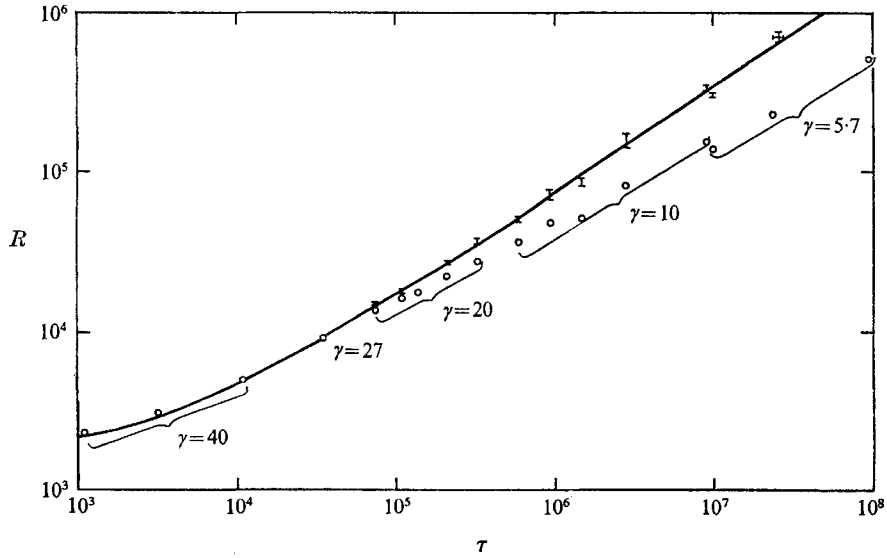

FIGURE 5. The Rayleigh numbers R_c, R_k, recalculated from Rossby's data, as a function of the Taylor number τ; O, R_c; I, R_k, —, Chandrasekhar's marginal stability curve.

$\tau \times 10^{-4}$	$R_c \times 10^{-3}$	γ	A	$\lambda \times 10^3$
0·11	2·3	40	244	0·85
0·32	3·1	40	98	1·4
1·1	5·0	40	24	3·6
3·5	9·4	28	32	2·8
7·5	14	20	62	1·6
11	16	20	43	2·2
14	18	20	43	2·2
21	22	20	22	3·7
34	28	20	13	5·0
60	36	10	120	1·0
95	48	10	71	1·4
150	50	10	45	1·8
286	80	10	25	4·6
900	150	10	7·3	8·3
1000	135	5·7	63	1·5
2400	225	5·7	24	2·9
9690	500	5·7	6·5	13·2

TABLE 2. Stability parameters calculated from Rossby's data

fixed Taylor number the region near the side wall would first become unstable at a subconductive value of the Rayleigh number. This Rayleigh number should depend on λ, and therefore, the fluid depth. However, Rossby finds that the critical Rayleigh number is approximately independent of height. If convective effects are to explain the data, the dependence on λ would have to be small in the region of parameter space under consideration. As the side regions convected heat, the Nusselt number would rise slightly with increasing imposed temperature difference. This rise would be limited due to the small horizontal area of the convection region. At some larger value of the Rayleigh number, the entire interior region, over which the similarity solution holds, would become unstable; there would be a corresponding increase both in the Nusselt number and the slope of the Nu–R curve, since larger regions would be convecting heat. Until the interior region becomes unstable, the Nusselt number based on total horizontal area would be a function of fluid depth as well as Rayleigh number, since the horizontal area available to convective heat transfer varies linearly with depth. Five aspect ratios were studied by Rossby and these are indicated in figure 5. At a given aspect ratio, centrifugal effects should become more important with increasing Taylor number since λ increases with τ. Considering all the data, the aspect ratio decreases as the Taylor number increases, and according to figure 3 this should cause a slight increase in the effect of the centrifugal circulation on the critical Rayleigh number. Our analysis is in qualitative agreement with Rossby's data on these points. However, the analysis predicts that the critical Rayleigh number for the convective basic state is $O(\lambda^2)$ below that for the conductive basic state, and this difference is much smaller than the 30 % observed by Rossby. It would be of interest to extend the analysis to the region of parameter space investigated by Rossby, as well as to investigate baroclinic type instabilities and finite-amplitude instabilities of the centrifugally driven basic state.

Grateful acknowledgement is made to the National Science Foundation for partial support of this research through grant number NSF GK 2505 and an NSF Traineeship held by G. M. Homsy.

REFERENCES

Barcilon, V. & Pedlosky, J. 1967*a* *J. Fluid Mech.* **29**, 609.
Barcilon, V. & Pedlosky, J. 1967*b* *J. Fluid Mech.* **29**, 673.
Chandrasekhar, S. 1961 *Hydrodynamic and Hydromagnetic Stability*. Clarendon.
Courant, R. & Hilbert, D. 1953 *Methods of Mathematical Physics*, vol. 1. Interscience.
Fox, L. 1962 *Numerical Solution of Ordinary and Partial Differential Equations*. Pergamon.
Homsy, G. M. 1969 Ph.D. Thesis, University of Illinois.
Homsy, G. M. & Hudson, J. L. 1969 *J. Fluid Mech.* **35**, 33.
Homsy, G. M. & Hudson, J. L. 1971 *J. Fluid Mech.* **45**, 353.
Koschmieder, E. L. 1966 *Beitr. Phys. Atmos.* **39**, 208.
Koschmieder, E. L. 1967 *Beitr. Phys. Atmos.* **40**, 216.
Küppers, G. & Lortz, D. 1969 *J. Fluid Mech.* **35**, 609.
Müller, U. 1966 *Beitr. Phys. Atmos.* **39**, 217.
Niiler, P. & Bisshopp, F. E. 1965 *J. Fluid Mech.* **22**, 753.
Rossby, H. T. 1969 *J. Fluid Mech.* **36**, 309.
Veronis, G. 1968 *J. Fluid Mech.* **31**, 113.
Watson, P. 1968 *J. Fluid Mech.* **32**, 399.